Int. J. Heat Mass Transfer. Vol. 20, pp. 23–30. Pergamon Press 1977. Printed in Great Britain

LAMINAR FILM CONDENSATION OF FLOWING VAPOR ON A HORIZONTAL MELTING SURFACE

D. H. CHO and M. EPSTEIN
Argonne National Laboratory, Argonne, IL 60439, U.S.A.

(*Received* 17 *December* 1975 *and in revised form* 13 *April* 1976)

Abstract—Laminar film condensation of a saturated vapor flowing over a horizontal melting surface is studied analytically. Using an approximate treatment of the shear stress at the vapor–liquid interface (as suggested by Shekriladze and Gomelauri), the similarity conservation equations are solved numerically. Solutions for the condensation rate, melting rate and skin friction are obtained for three values of the liquid Prandtl number (0.1, 1 and 10) and for a wide range of condensation and melting parameters (Stefan numbers). The solutions become exact as the parameter $[(\rho\mu)/(\rho_v\mu_v)]^{1/2}$ goes to infinity. Simple analytical solutions based on a thin-film approximation are also derived and compared with the numerical results.

NOMENCLATURE

c, specific heat;
F, dimensionless stream function; equation (2);
k, thermal conductivity;
L_f, heat of fusion;
L_v, heat of vaporization;
$\dot{m}_s$, local melting rate per unit area;
$\dot{m}_v$, local condensation rate per unit area;
N_1, condensation parameter, $c(T_v - T_{mp})/L_v$, equation (23);
N_2, melting parameter, $c(T_v - T_{mp})/[L_f + c_s(T_{mp} - T_0)]$, equation (15);
Pr, liquid Prandtl number, $c\mu/k$;
Re_f, film Reynolds number, $4\delta\langle u\rangle\rho/\mu$;
Re_x, Reynolds number, $u_\infty x/\nu$;
T, temperature;
u, velocity component in x-direction;
$\langle u\rangle$, average film velocity in x-direction;
u_∞, free stream velocity of vapor;
v, velocity component in y-direction;
x, coordinate measuring distance along the melting surface from the leading edge;
y, coordinate measuring distance normal to the melting surface.

Greek symbols

δ, liquid film thickness;
η, similarity variable; equation (1);
η_δ, dimensionless liquid film thickness;
θ, dimensionless temperature; $(T - T_{mp})/(T_v - T_{mp})$; equation (3);
μ, absolute viscosity;
ν, kinematic viscosity;
ρ, density;
ψ, stream function;
τ_w, shear stress at the melting surface.

Subscripts

mp, melting point;
0, condition in the solid far from the melting surface;
s, solid;
v, vapor.

1. INTRODUCTION

WHEN a condensing vapor comes into contact with a solid surface, the surface may melt while the vapor condenses on it. Such simultaneous condensation and melting will occur when the vapor temperature is higher than the melting point of the solid. This problem is complicated by the fact that the liquid film is formed by both condensation of the vapor and melting of the solid. In fact, more liquid comes from melting than condensation because the heat of fusion is considerably less than the heat of vaporization. The problem has considerable practical significance in certain engineering applications. For example, in the freeze-desalination process, ice is melted by condensing a refrigerant vapor onto the ice surface [1]. Steam jets are used in some applications to remove or drill through high ice-content soils [2]. Also, the melting attack of structural materials by metal vapors or ceramic fuel vapors is of interest in safety studies of fast breeder nuclear reactors [3].

Laminar film condensation of a pure vapor onto a vertical melting surface, where the liquid flow is generated by gravity forces, was first analyzed by Tien and Yen [4]. Later, Yen *et al.* [5] extended the analysis to examine the effect of noncondensable gases on the condensation-melting heat transfer. In both studies, it was assumed that the condensing vapor and the melting solid are of the same material and that the Prandtl number of the material is much greater than unity. Recently, Epstein and Cho performed an analysis [6] which allows for the possibility that the condensing vapor and the melting solid are of different materials of immiscible liquids and accounts for the effects of both liquid film inertia and shear at the interface between the condensing vapor and liquid film.

In the studies mentioned above, the velocity of the condensing vapor was taken to be zero so that gravity was the only force removing the liquid layers formed by condensation and melting. As a first step toward examining the effect of the vapor velocity, this paper considers laminar film condensation of a saturated vapor flowing over a horizontal melting surface. The mathematical formulation of the problem is similar to

the boundary-layer analysis developed by Koh [7] for laminar-film condensation in forced flow over a flat plate, except that we allow for mass addition at the solid surface due to melting. Following the treatment suggested by Shekriladze and Gomelauri [8], the shear stress at the vapor–liquid interface was approximated by the momentum given up by the condensing vapor. Using a marching integration technique (trial-and-error method), the resulting similarity equations were solved numerically for one-component systems in which the condensing vapor and the melting solid are of the same material. Solutions were obtained for three values of the liquid Prandtl number ($Pr = 0.1$, 1, 10) with a wide range of condensation and melting parameters. The numerical (exact) results were compared with simple analytical solutions based on a thin-film approximation.

2. ANALYSIS

Physical model

A schematic diagram of the physical model and coordinate system is presented in Fig. 1. A stream of pure vapor at a velocity u_∞ is flowing over a horizontal melting surface. The vapor is saturated at temperature T_v. The temperature at the melting surface corresponds to the melting point of the solid T_{mp} while the temperature of the solid far from the melting surface is maintained at $T_0 (T_0 < T_{mp})$. It is assumed that in steady state, the liquids from melting and condensation flow side by side as a smooth (laminar) composite film. At

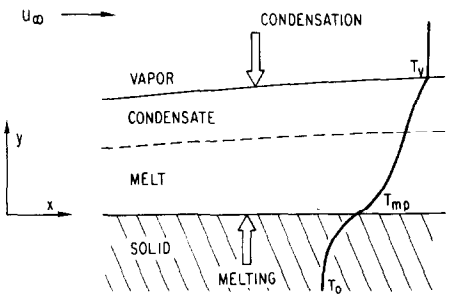

FIG. 1. Physical model and coordinate system.

the melting surface, the liquid velocity in the direction of vapor flow is zero. Away from the melting surface, the liquid film moves under the influence of drag forces due to the vapor flow. The heat released from vapor condensation is divided among energy convection by the moving liquid film, melting of the solid, and heat conduction into the solid. The coordinate system is fixed to the melting surface, so the solid material appears to be moving toward the film with a mass flux corresponding to the melting rate. While the melting rate is a function of x, it is assumed here that the geometry change of the melting surface can be neglected.* In addition, as is usual in simple condensation theory, we neglect effects related to liquid–film surface instabilities. Finally, physical properties that appear in the governing equations are considered to be constant.

*The validity of this assumption is discussed in [6].

Governing equations

The basic governing partial differential equations for the liquid film have been given elsewhere (see, for example [9]) and need not be repeated here. The partial differential equations can be transformed into a corresponding set of ordinary differential equations, using the following similarity transformation:

$$\eta = y\sqrt{\left(\frac{u_\infty}{\nu x}\right)} \tag{1}$$

$$\psi = F\sqrt{(\nu u_\infty x)} \tag{2}$$

$$\theta = \frac{T - T_{mp}}{T_v - T_{mp}} \tag{3}$$

$$u = \frac{\partial \psi}{\partial y} = u_\infty F'(\eta) \tag{4}$$

$$v = -\frac{\partial \psi}{\partial x} = \tfrac{1}{2}\sqrt{\left(\frac{\nu u_\infty}{x}\right)}(-F + \eta F'). \tag{5}$$

The momentum and energy equations for the liquid film then become, respectively,

$$F''' + \tfrac{1}{2}FF'' = 0 \tag{6}$$

$$\theta'' + \tfrac{1}{2}PrF\theta' = 0 \tag{7}$$

where the prime denotes differentiation with respect to η.

The boundary conditions at the melting surface ($y = 0$) are:

$$\text{at } y = 0, \quad u = 0 \tag{8}$$

$$T = T_{mp} \tag{9}$$

$$k\left(\frac{\partial T}{\partial y}\right) = L_f \rho v + c_s(T_{mp} - T_0)\rho v. \tag{10}$$

Since our coordinate system is fixed to the melting surface, the solid material appears to be moving toward the liquid film at the local melting rate, which is given by

$$\dot{m}_s = \rho v(y = 0). \tag{11}$$

Equation (10) states that the heat conducted to the melting surface is equal to the heat of melting plus the sensible heat required to raise the solid temperature to the melting point. In terms of the transformed variables, equations (8)–(10) become

$$\text{at } \eta = 0, \quad F' = 0 \tag{12}$$

$$\theta = 0 \tag{13}$$

$$N_2\theta' + \tfrac{1}{2}PrF = 0 \tag{14}$$

where N_2 is the melting parameter defined by

$$N_2 = \frac{c(T_v - T_{mp})}{L_f + c_s(T_{mp} - T_0)}. \tag{15}$$

The boundary conditions at the condensing surface ($y = \delta$) are:

$$\text{at } y = \delta, \quad \nu\frac{\partial u}{\partial y} = (u - u_\infty)(-\dot{m}_v/\rho) \tag{16}$$

$$T = T_v \tag{17}$$

$$k\frac{\partial T}{\partial y} = L_v \dot{m}_v \tag{18}$$

where $\dot{m}_v$ is the vapor condensation rate per unit area and is given by

$$\dot{m}_v = -\rho\left(v - u\frac{\mathrm{d}\delta}{\mathrm{d}x}\right)_{y=\delta}. \tag{19}$$

In terms of the transformed variables, equations (16)–(18) become

$$\text{at } \eta = \eta_\delta, \quad F'' + \tfrac{1}{2}FF' - \tfrac{1}{2}F = 0 \tag{20}$$

$$\theta = 1 \tag{21}$$

$$N_1\theta' - \tfrac{1}{2}PrF = 0 \tag{22}$$

where N_1 is the condensation parameter defined by

$$N_1 = \frac{c(T_v - T_{mp})}{L_v}. \tag{23}$$

Equation (16) states that the shear force at the vapor–liquid interface is equal to the momentum given up by the condensing vapor. This shear condition is an approximation proposed by Shekriladze and Gomelauri [8]. It corresponds to an asymptotic solution of the vapor momentum boundary-layer equation in the limit of strong suction. Exact treatment of the interfacial shear would require simultaneous consideration of both liquid and vapor boundary layers, as was done by Koh [7]. The shear approximation has been used by a number of investigators [10, 11]. In particular, the accuracy of the shear approximation has been investigated by Denny and Mills for the case of combined gravity and forced flow [10]. Denny and Mills have found that for the range of variables considered in their investigation, the error in the heat transfer introduced by the shear approximation is less than 1% for

$$\frac{\dot{m}_v}{\rho_v u_\infty}\sqrt{\left(\frac{xu_\infty}{v_v}\right)} > 2 \tag{24}$$

where ρ_v and v_v are the vapor density and kinematic viscosity, respectively. The criterion may be rewritten as

$$\left(\frac{\rho\mu}{\rho_v\mu_v}\right)^{1/2}\frac{\dot{m}_v}{\rho u_\infty}\left(\frac{xu_\infty}{v}\right)^{1/2} > 2 \tag{25}$$

or, in terms of the transformed variables, it takes the form

$$\left(\frac{\rho\mu}{\rho_v\mu_v}\right)^{1/2}\frac{N_1}{Pr}\theta'(\eta_\delta) > 2 \tag{26}$$

where μ_v is the vapor viscosity. A similar conclusion may be obtained from Cess's analysis of laminar film condensation in a forced flow over a flat plate [9]. This analysis, which neglected inertia forces and energy convection, indicates that the shear approximation is valid for $[(\rho\mu)/(\rho_v\mu_v)]^{1/2}(N_1/Pr) \gg 1$ (say, for $[(\rho\mu)/(\rho_v\mu_v)]^{1/2}(N_1/Pr) > 4$; see Fig. 3 of [9]). Thus it would be expected that the shear approximation would be reasonable for most engineering applications involving high condensation rates.

The governing equations (6)–(7) combined with the boundary conditions (12)–(14) and (20)–(22) suffice to provide solutions as function of three physical parameters N_1, N_2, and Pr. Once the governing equations are solved, the local condensation rate, melting rate, and skin friction can be computed as follows.

Dimensionless condensation rate

$$\frac{\dot{m}_v}{\rho u_\infty}(Re_x)^{1/2} = \frac{N_1}{Pr}\theta'(\eta_\delta) = \frac{F(\eta_\delta)}{2} \tag{27}$$

Dimensionless melting rate

$$\frac{\dot{m}_s}{\rho u_\infty}(Re_x)^{1/2} = \frac{N_2}{Pr}\theta'(0) = -\frac{F(0)}{2} \tag{28}$$

Dimensionless skin friction

$$\frac{\tau_w}{\rho u_\infty^2}(Re_x)^{1/2} = F''(0) \tag{29}$$

where $Re_x = xu_\infty/v$ and $\tau_w = \mu(\partial u/\partial y)_{y=0}$. The average condensation and melting rates over a distance x are equal to twice the corresponding local values at x.

Method of solution

A trial-and-error marching integration technique was employed. Numerical integration was performed using a library program available at the Applied Mathematics Division of Argonne National Laboratory (based on the Gear method [12]). For a given Prandtl number, the solution procedure was as follows. First, solve the momentum equation (6) with assumed values for $F(0)$ and $F''(0)$ and determine those solutions which satisfy the shear stress condition at η_δ, equation (20) (η_δ need not be specified, however). Second, solve the energy equation (7) with these momentum solutions and compute N_2 and N_1 using equations (14) and (22), respectively. Third, select those solutions which give desired values of N_1 and N_2 within an error bound of 2%.

Thin-film approximation

Before we discuss the numerical solutions, it seems useful to consider the case when the inertia forces and energy convection effects may be neglected. In this case, solution of the momentum and energy equations gives linear velocity and temperature profiles in the liquid film. The appropriate film thickness and coefficients are determined using the boundary conditions (12)–(14) and (20)–(22). It can then be shown that the local condensation rate, melting rate, and skin friction are given as follows.

Dimensionless condensation rate

$$\frac{\dot{m}_v}{\rho u_\infty}(Re_x)^{1/2} = \frac{N_1/Pr}{2\left(1+\dfrac{N_1}{Pr}\right)^{1/2}\left(1+\dfrac{N_2}{N_1}\right)^{1/2}} \tag{30}$$

Dimensionless melting rate

$$\frac{\dot{m}_s}{\rho u_\infty}(Re_x)^{1/2} = \frac{N_2/Pr}{2\left(1+\dfrac{N_1}{Pr}\right)^{1/2}\left(1+\dfrac{N_2}{N_1}\right)^{1/2}} \tag{31}$$

Dimensionless skin friction

$$\frac{\tau_w}{\rho u_\infty^2}(Re_x)^{1/2} = \frac{N_1/(Pr+N_1)}{2\left(1+\dfrac{N_1}{Pr}\right)^{1/2}\left(1+\dfrac{N_2}{N_1}\right)^{1/2}}. \tag{32}$$

The dimensionless heat flux at the melting wall is given by

$$\theta'(0) = \frac{1}{2\left(1+\frac{N_1}{Pr}\right)^{1/2}\left(1+\frac{N_2}{N_1}\right)^{1/2}}. \quad (33)$$

It is easy to see that in the absence of melting ($N_2 = 0$), equation (33) reduces to Shekriladze and Gomelauri's solution for pure condensation (equation (8) of [8]) and checks with Cess's limiting solution for $[(\rho\mu)/(\rho_v\mu_v)]^{1/2}(N_1/Pr) \gg 1$ when $N_1 \ll 1$ (equation (27) of [9]).

Another thin-film approximation is also possible, although its practical usefulness is limited. Cess's analysis [9] indicates that the interfacial shear may be approximated by the dry friction, i.e. friction over a solid surface without condensation, when

$$[(\rho\mu)/(\rho_v\mu_v)]^{1/2}(N_1/Pr)$$

is of the order of 0.1 or less. In this case, the dimensionless skin friction is given by $F''(0) = F''(\eta_\delta) = 0.332\,[(\rho_v\mu_v)/(\rho\mu)]^{1/2}$. Using this shear condition along with the boundary conditions (12)–(14) and (21)–(22), it can be shown that the dimensionless heat flux is given by

$$\theta'(0) = \theta'(\eta_\delta) = \left(\frac{a}{2}\right)^{1/3}\left(\frac{Pr}{N_2}\sqrt{\left[1+\frac{N_1}{N_2}\right]}\right)^{1/3}\left(1+\frac{N_1}{N_2}\right)^{-1/2} \quad (34)$$

where $a = 0.166\,[(\rho_v\mu_v)/(\rho\mu)]^{1/2}$. In the absence of melting ($N_2 = 0$), equation (34) reduces to Cess's limiting solution for $[(\rho\mu)/(\rho_v\mu_v)]^{1/2}(N_1/Pr) \ll 1$ (equation (26) of [9]). Using equation (34), the local condensation and melting rate may be obtained from equations (27) and (28).

It may be noted that the thin-film approximation can be easily extended to derive simple analytical solutions for the case where the condensing vapor and the melting solid are of different materials of immiscible liquids [13].

3. RESULTS AND DISCUSSION

To examine the accuracy of the shear approximation used in the present study, calculations have been performed for the case of no melting ($N_2 = 0$). Figure 2 compares the results with Koh's exact solutions [7]* for $[(\rho\mu)/(\rho_v\mu_v)]^{1/2} = 500$,† which are indicated by broken curves. The dimensionless wall heat flux, $\theta'(0)$, is plotted against the condensation parameter N_1. As would be expected from the criterion given by (26), our solutions are very close to Koh's solutions for $N_1/Pr = c(T_v - T_{mp})/(PrL_v) > 0.01$. For $Pr = 1$ and 10,

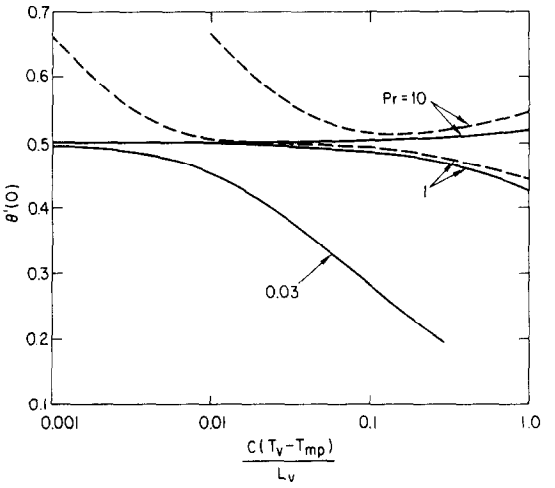

FIG. 2. Heat flux at the wall in the absence of melting; the present solutions (solid curves) are compared with Koh's exact solutions for $[(\rho\mu)/(\rho_v\mu_v)]^{1/2} = 500$ (broken curves).

however, our solutions tend to deviate somewhat from Koh's solutions as N_1/Pr becomes large. This deviation for high Prandtl numbers is not understood. For $Pr = 0.03$, it is not possible to distinguish our solutions from Koh's solutions as given in Fig. 7(a) of [7]. Therefore, it would appear that unless the Prandtl number is very large, the shear approximation given by equation (16) is reasonable for many realistic values of the condensation parameter.

The calculational results for simultaneous condensation and melting are presented in Figs. 3–11. Figures 3–5 show the local condensation rate as a function of the condensation parameter N_1 with the melting parameter N_2 as parameter for $Pr = 0.1$, 1,

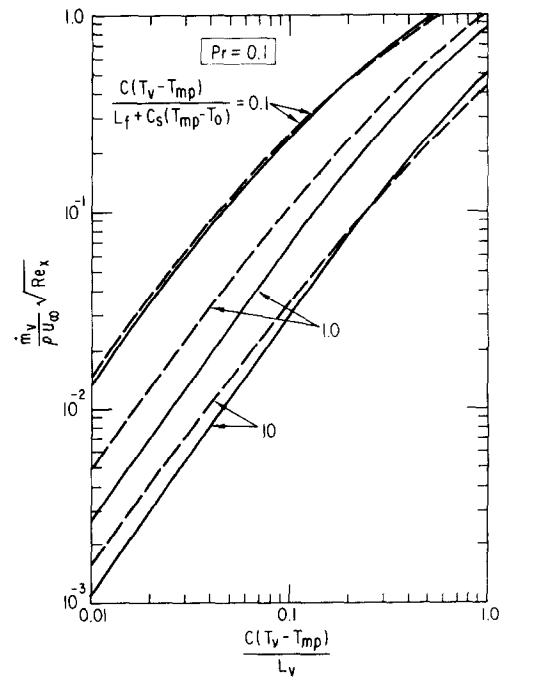

FIG. 3. Local condensation rates for $Pr = 0.1$ (broken curves indicate the thin-film approximation).

*Figure 7(b) of [7] appears to contain some mislabeling. The curves for $[(\rho\mu)/(\rho_v\mu_v)]^{1/2} = 100$ should have been for $[(\rho\mu)/(\rho_v\mu_v)]^{1/2} = 500$ and vice versa.

†As has been noted by Sparrow *et al.* [14], realistic values of the parameter $[(\rho\mu)/(\rho_v\mu_v)]^{1/2}$ range from 200 to 2000 for typical condensation processes at atmospheric pressure. Obviously, the shear approximation given by equation (16) becomes more accurate as the value of this parameter increases. In fact, it is exact when the parameter is infinitely large.

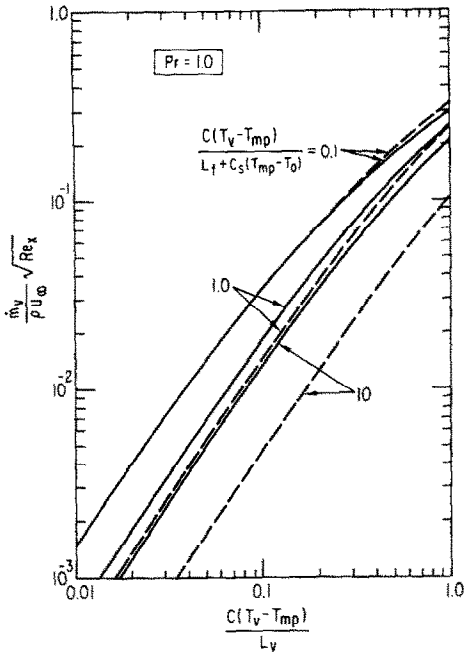

FIG. 4. Local condensation rates for $Pr = 1.0$ (broken curves indicate the thin-film approximation).

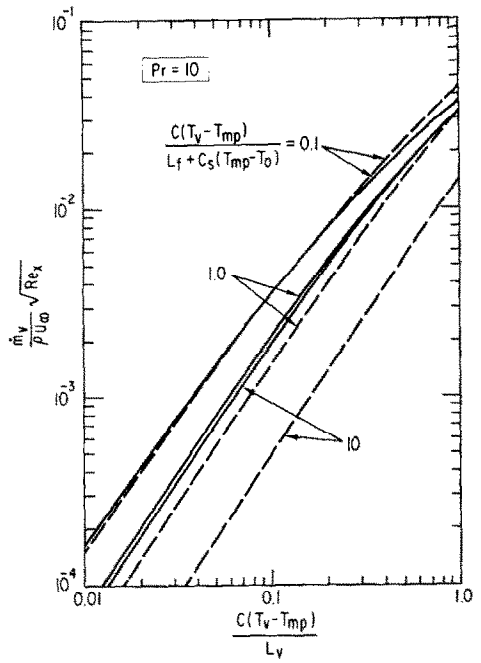

FIG. 5. Local condensation rates for $Pr = 10$ (broken curves indicate the thin-film approximation).

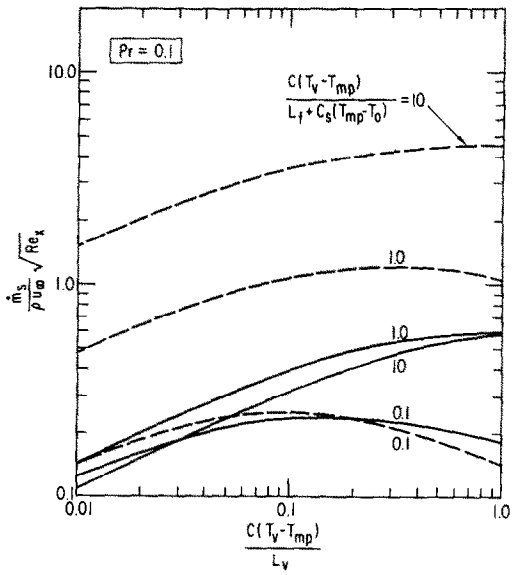

FIG. 6. Local melting rates for $Pr = 0.1$ (broken curves indicate the thin-film approximation).

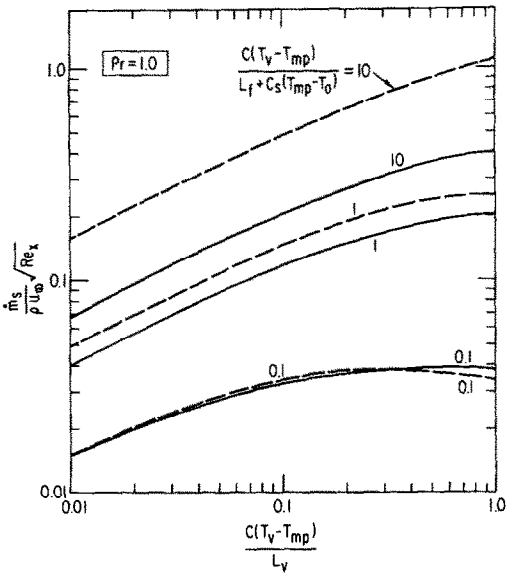

FIG. 7. Local melting rates for $Pr = 1.0$ (broken curves indicate the thin-film approximation).

and 10. Similarly, the local melting rates are given in Figs. 6–8 and the skin friction in Figs. 9–11. Also shown for comparison purposes are solutions based on the thin-film approximation corresponding to equations (30)–(32). The thin-film solutions are indicated by broken curves.

Turning first to Figs. 3–5, we find that the condensation rates decrease as the melting parameter N_2 increases. This would be expected, since melting increases the liquid film thickness, thereby reducing the temperature driving force for condensation. For a given melting parameter, the condensation rates increase with increasing condensation parameter N_1. This trend is not different from that for condensation without melting and requires no further explanations. For $Pr = 0.1$, the thin-film approximation appears to be reasonably good in estimating the condensation rates for a wide range of the melting parameter. For high Prandtl numbers, the effect of N_2 on the condensation rates appears to be somewhat reduced, and the thin-film approximation underestimates the condensation rates when the melting parameter is large. This behavior seems to be related to the blowing effect produced by melting. When viewed from our coordinate system, melting produces a normal velocity at the melting

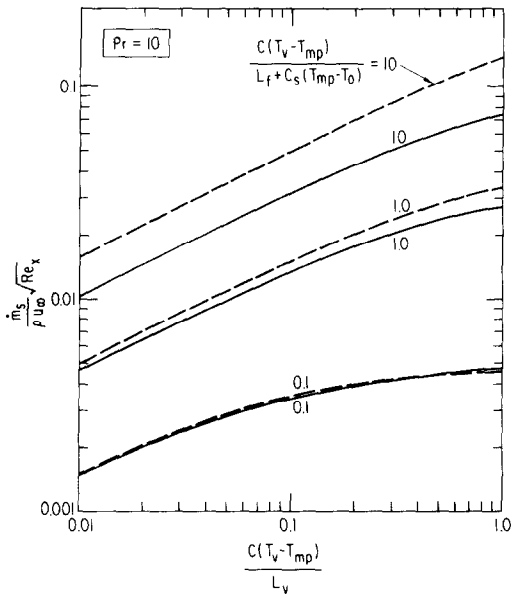

FIG. 8. Local melting rates for $Pr = 10$ (broken curves indicate the thin-film approximation).

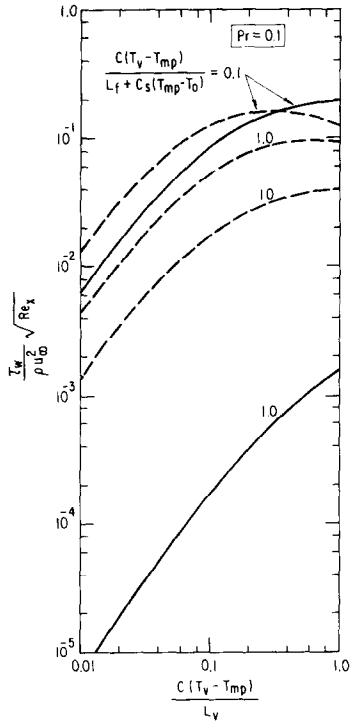

FIG. 9. Local skin friction for $Pr = 0.1$ (broken curves indicate the thin-film approximation).

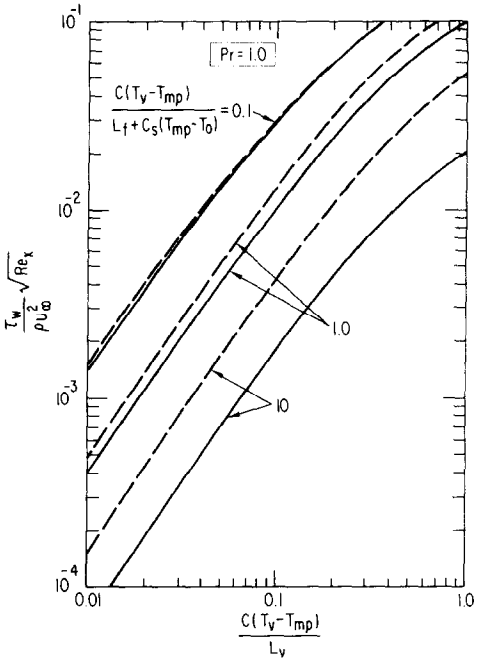

FIG. 10. Local skin friction for $Pr = 1.0$ (broken curves indicate the thin-film approximation).

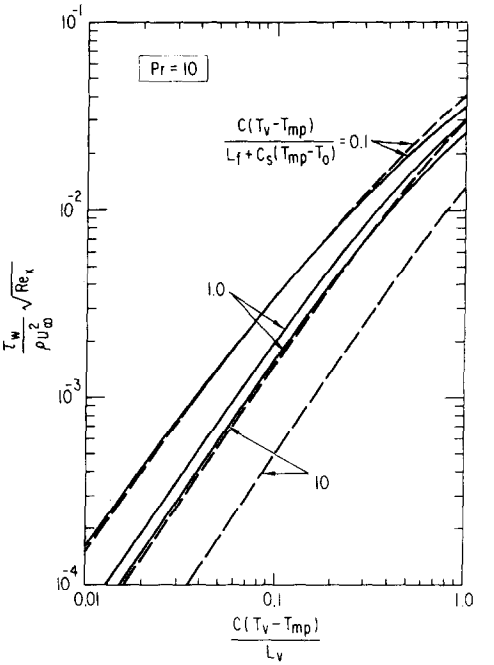

FIG. 11. Local skin friction for $Pr = 10$ (broken curves indicate the thin-film approximation).

surface. The melting velocity acts to reduce the steepness of the temperature gradient at the melting surface in a way similar to the blowing process in a boundary-layer flow [15, 16]. As a result, the melting rates will be reduced below the thin-film prediction, as will be seen later. It appears, however, that for $Pr = 1$ and 10, the blowing velocity increases the steepness of the temperature gradient at the condensing surface, thereby providing a larger driving force for condensation than predicted by the thin-film approximation. For $Pr = 0.1$, inertia effects are also very important, and it may thus be fortuitous that the thin-film approximation predicts the condensation rates reasonably well.

We now turn to the melting rates as shown in Figs. 6–8. Unless the melting parameter N_2 is very small, the melting rates generally increase with increasing condensation parameter N_1. This behavior differs from that observed for gravity-flow condensation and melt-

ing [6]. This is related to two competing effects. For a given N_2, increasing N_1 tends to increase the film thickness because of the increased condensation rates. On the other hand, the liquid film moves faster, since the shear force at the liquid–vapor interface increases with increasing condensation rate and thus its thickness tends to decrease. When N_2 is much greater than N_1, the latter effect is large enough to dominate. For $N_2 \ll N_1$, the former effect is more important and the melting rates may be estimated using heat-flux values for the case of no melting. It is seen that for $N_2 = 1$ and 10, the thin-film approximation overestimates the melting rates, the deviation increasing with increasing melting parameter. For $Pr = 1$ and 10, the deviation is due mainly to the blowing effect at the melting surface. However, the especially marked deviation for $Pr = 0.1$ is related to the inertia of the melt layer as well as the blowing effect. The inertia causes the melt layer to become thicker than predicted by the thin-film approximation* and, coupled with the blowing effect, greatly reduces the temperature gradient at the melting surface. In fact, the inertia effects for $Pr = 0.1$ are so strong that the melting rates are seen to decrease slightly as N_2 is increased from 1 to 10. This somewhat unexpected behavior would only be of academic interest, because, as will be discussed later, the applicability of the present laminar analysis is very limited for this parameter range.

Figures 9–11 show the dimensionless skin friction at the melting surface, $F''(0)$, as a function of N_1 with N_2 as parameter. It is seen that the skin friction increases with increasing condensation parameter N_1. This is expected, since the shear force that moves the liquid film increases with increasing condensation rate. The skin friction is found to decrease with increasing melting parameter N_2. As has been observed in Figs. 7 and 8, for $Pr = 1$ and 10, the melting velocity increases with increasing melting parameter. Thus, the effect of increasing N_2 on the skin friction is similar to the effect of blowing in a forced-convection, boundary-layer flow [15]. However, the dramatic decrease in skin friction for $Pr = 0.1$ largely represents the strong inertia effects of the melt layer. (The results for $N_2 = 10$, which lie outside the range of scale of Fig. 9, would be of little practical interest.)

It should be noted that since $L_v > L_f + c_s(T_{mp} - T_0)$ for most materials, the foregoing analytical results for parameter values $N_1 > N_2$ are of little practical significance. More important, the results are valid only when the film is moving in laminar flow with straight streamlines. The nature of the flow changes with the film Reynolds number, which is defined by $Re_f = 4\delta\langle u\rangle\rho/\mu$ where $\langle u\rangle$ is the average film velocity. For water condensing on a vertical surface, waves appear at Re_f of about 30, and a transition to turbulent flow occurs at Re_f between 300 and 2000 [10]. Using these values of Re_f, we shall examine the region of validity of the present results. To do this, the film Reynolds number has been derived based on the thin-film approximation. It is given by

$$Re_f = 4(Re_x)^{1/2}\left(\frac{N_1}{Pr+N_1}\right)\left(1+\frac{N_1}{Pr}\right)^{1/2}\left(1+\frac{N_2}{N_1}\right)^{1/2}. \tag{35}$$

Consider, for example, saturated steam at atmospheric pressure condensing on ice at its melting point. Using $N_1 = 0.185$, $N_2 = 1.25$, and $Pr = 7.0$, it is found that $Re_f = 0.29(Re_x)^{1/2}$. Thus, surface waves will appear on the film when $Re_x = 1.1 \times 10^4$ and the flow becomes turbulent when $Re_x = 1.1 \times 10^6 \sim 4.8 \times 10^7$. For $u_\infty = 10$ m/s ($\sim$30 ft/s), surface waves will appear at $x = 1.2$ mm and the transition to turbulent flow will occur at $x = 0.12$–4.8 m. When values of N_1/Pr and/or N_2/Pr are greater than unity, the applicability of the present laminar analysis is quite limited. For the melting attack of steel structure by steel vapor (which may occur in a core disruptive accident of liquid-metal-cooled fast-breeder reactors), typical values of N_1/Pr and N_2/Pr are 1 and 10, respectively. In this case, the transition to turbulent flow occurs when $Re_x = 10^3 \sim 4.5 \times 10^4$, the corresponding value of x for $u_\infty = 10$ m/s being somewhere between 0.1 and 4.5 mm. These values of x would be an underestimate, since the thin-film approximation on which equation (35) is based overestimates the melting rate for this case. The above calculation, however, clearly indicates the limited applicability of the present analysis when values of N_1/Pr and/or N_2/Pr exceed unity. Strictly speaking, the present analysis is considered to be valid when the flow is laminar and no surface waves are present. The presence of surface waves will cause an increase in heat transfer. The present analytical results provide a basis for the empirical correlation of the effects of surface waves. In the absence of reliable analyses of turbulence effects, the present results can even prove to be useful in correlating heat-transfer data for turbulent films. Unfortunately, no experimental data is available for comparison with the present analytical results. However, it may be mentioned in passing that the melting heat-transfer coefficients which were measured in experiments involving gravity-flow steam condensation on a vertical ice plate in the presence of air [5] and a melting ice sphere in a warm laminar liquid flow [18], were found to be in good agreement with theoretical predictions based on boundary-layer analyses similar to the present analysis.

Acknowledgements—It is a pleasure to acknowledge Mr. F. Pellett for his assistance in the programming and computational stages of this research.

This work was performed under the auspices of the U.S. Energy Research and Development Administration.

*Similar inertia effects occur in the melting of solid bodies immersed in hot fluid flows when the Prandtl number is low [17].

REFERENCES

1. P. A. Weiss, Desalination by freezing, in *Practice of Desalination* (edited by R. Bakish), pp. 260–270. Noyes Data Corp., New Jersey (1973).
2. S. M. Hodge, Instruments and methods; a new version of a steam-operated ice drill, *J. Glaciol.* **10**(60), 387–393 (1971).

3. M. Epstein and D. H. Cho, Melting rates for the attack of steel structure by UO_2 fuel or steel vapor, *Trans. Am. Nucl. Soc.* **21**, 311 (1975).
4. C. Tien and Y. C. Yen, Condensation-melting heat transfer, *Chem. Engng Progr. Symp. Ser.* No. 113 **67**, 1–9 (1971).
5. Y. C. Yen, A. Zehnder, S. Zavoluk and C. Tien, Condensation-melting heat transfer in the presence of air, *Chem. Engng Progr. Symp. Ser.* No. 131 **69**, 23–29 (1973).
6. M. Epstein and D. H. Cho, Laminar film condensation on a vertical melting surface, *J. Heat Transfer* **98C**, 108–113 (1976).
7. J. C. Y. Koh, Film condensation in a forced-convection boundary-layer flow, *Int. J. Heat Mass Transfer* **5**, 941–954 (1962).
8. I. G. Shekriladze and V. I. Gomelauri, Theoretical study of laminar film condensation of flowing vapor, *Int. J. Heat Mass Transfer* **9**, 581–591 (1966).
9. R. D. Cess, Laminar-film condensation on a flat plate in the absence of a body force, *Z. Angew. Math. Phys.* **11**, 426–433 (1960).
10. V. E. Denny and A. F. Mills, Nonsimilar solutions for laminar film condensation on a vertical surface, *Int. J. Heat Mass Transfer* **12**, 965–979 (1969).
11. H. Honda and T. Fujii, Effect of the direction of oncoming vapor on laminar filmwise condensation on a horizontal cylinder, in *Proceedings of the Fifth International Heat Transfer Conference*, Tokyo, Japan, Vol. III, pp. 299–303. A.I.Ch.E., New York (1974).
12. C. W. Gear, The numerical integration of ordinary differential equations of various orders, Argonne National Laboratory Report, ANL-7126 (1966).
13. D. H. Cho and M. Epstein, Melting of steel structure by flowing fuel or steel vapor, *Trans. Am. Nucl. Soc.* **22**, 386–387 (1975).
14. E. M. Sparrow, W. J. Minkowycz and M. Saddy, Forced convection condensation in the presence of noncondensables and interfacial resistance, *Int. J. Heat Mass Transfer* **10**, 1829–1845 (1967).
15. J. P. Hartnett and E. R. G. Eckert, Mass-transfer cooling in a laminar boundary layer with constant fluid properties, *Trans. Am. Soc. Mech. Engrs* **79**, 247–254 (1957).
16. Y. C. Yen and C. Tien, Laminar heat transfer over a melting plate, the modified Leveque problem, *J. Geophys. Res.* **68**(12), 3673–3678 (1963).
17. M. Epstein and D. H. Cho, Melting heat transfer in steady laminar flow over a flat plate, *J. Heat Transfer* **98C**, 531–533 (1976).
18. F. M. Pozvonkov, E. F. Shurgalskii and L. S. Akselrod, Heat transfer at a melting flat surface under conditions of forced convection and laminar boundary layer, *Int. J. Heat Mass Transfer* **13**, 957–962 (1970).

CONDENSATION LAMINAIRE EN FILM D'UNE VAPEUR S'ECOULANT SUR UNE SURFACE HORIZONTALE EN FUSION

Résumé—On étudie par voie analytique la condensation laminaire en film d'une vapeur saturée balayant une surface horizontale en fusion. Les équations de conservation formulées en similitude ont été résolues numériquement en utilisant un traitement approché de la tension de cisaillement de l'interface liquide–vapeur (méthode suggérée par Shekriladze et Gomelauri). Le taux de condensation, les taux de fusion et le frottement pariétal ont été obtenus pour trois valeurs du nombre de Prandtl du liquide (0,1–1 et 10) et pour un domaine étendu de paramètres de condensation et de fusion (nombres de Stefan). Les solutions sont exactes lorsque le paramètre $[(\rho\mu)/(\rho_v\mu_v)]^{1/2}$ tend vers l'infini. Des solutions analytiques simples basées sur l'approximation du film mince ont également été obtenues et comparées aux résultats numériques.

LAMINARE FILMKONDENSATION STRÖMENDEN DAMPFES AUF EINER HORIZONTALEN SCHMELZENDEN OBERFLÄCHE

Zusammenfassung—Die laminare Filmkondensation eines über eine horizontale schmelzende Oberfläche strömenden, gesättigten Dampfes wird analytisch untersucht. Unter Verwendung eines Näherungsansatzes für die Schubspannung an der Dampf–Flüssigkeits-Grenzfläche (entsprechend dem Vorschlag von Shekriladze und Gomelauri) werden die Erhaltungsgleichungen numerisch gelöst. Für drei Werte der Flüssigkeits-Prandtl–Zahl (0,1; 1 und 10) und für einen weiten Bereich von Kondensations- und Schmelzparametern (Stefan–Zahlen) werden Lösungen für die Kondensations- und Schmelzrate sowie für die Oberflächenreibung angegeben. Die Lösungen werden exakt, wenn Parameter $[(\rho\mu)/(\rho_v\mu_v)]^{1/2}$ gegen unendlich geht. Außerdem werden einfache analytische, auf einer Dünnschicht-Näherung beruhende Lösungen abgeleitet und mit den numerischen Werten verglichen.

ЛАМИНАРНАЯ ПЛЕНОЧНАЯ КОНДЕНСАЦИЯ ПАРА, ТЕКУЩЕГО ПО ГОРИЗОНТАЛЬНОЙ ПОВЕРХНОСТИ ПЛАВЛЕНИЯ

Аннотация — Аналитически исследуется ламинарная пленочная конденсация насыщенного пара, текущего по горизонтальной поверхности плавления. С помощью приближенного представления напряжений сдвига на поверхности раздела пар-жидкость (предложенной Шекриладзе и Гомелаури) решались численно автомодельные уравнения сохранения. Решения для скорости конденсации, плавления и поверхностного трения получены для трех значений чисел Прандтля для жидкости (0,1; 1 и 10) и широкого диапазона параметров конденсации и плавления (числа Стефана). Решения становятся точными, когда параметр $[(\rho\mu)/(\rho_v\mu_v)]^{1/2}$, стремится к бесконечности. С помощью приближения тонкой пленки получены простые аналитические решения, которые сравниваются с численными результатами.